Chapter 7
Triboluminescence of Lanthanide Complexes

Miki Hasegawa and Yasuchika Hasegawa

Abstract The photoluminescence of lanthanide complexes originating from f–f transitions is generally sensitized through energy transfer from the ligand to the lanthanide ion in the excited state under UV irradiation. This phenomenon is known as the photo-antenna effect. Luminescence driven by mechanical stimuli, such as tapping or rubbing, is called mechanoluminescence or triboluminescence (TL). In recent years, reports on TL in rare-earth complexes, which have attracted attention as novel luminescent materials that do not require an electrical excitation source, have steadily increased. In this chapter, we focus on triboluminescent lanthanide complexes. Specifically, we introduce the history and detection methods of TL and cite recent examples of materials demonstrating this phenomenon, particularly coordination polymer-like and discrete molecular crystalline lanthanide complexes. Finally, we summarize the application prospects of these complexes as soft crystals.

Keywords Triboluminescence · Lanthanide complexes · Crystal structure · Coordination polymer · Mechanical luminescence

7.1 Introduction

Changes in state from solid to liquid to gas occur as energy is absorbed and released. The single crystal–single crystal and crystal–amorphous phase transitions of molecular systems, such as soft crystals, as well as their chromic behavior, have recently been observed [1]. Mechanical stimulation can induce chemical changes by providing pressure-induced stimuli [2, 3] and changes in energy between excited states during electronic transition [4–8]. Especially in the case of molecular crystals, electronic absorption and emission bands are induced by changes in the distortion

M. Hasegawa (✉)
Department of Science and Engineering, College of Science and Engineering, Aoyama Gakuin University, 5-10-1 Fuchinobe, Chuo-Ku, Sagamihara-Shi, Kanagawa 252-5258, Japan
e-mail: hasemiki@chem.aoyama.ac.jp

Y. Hasegawa
Division of Applied Chemistry, Faculty of Engineering, Hokkaido University, Kita 13, Nishi 8, Kita-Ku, Sapporo 060-8628, Hokkaido, Japan

M. Kato and K. Ishii (eds.), *Soft Crystals*, The Materials Research Society Series,
https://doi.org/10.1007/978-981-99-0260-6_7

or co-planarity of π-electronic systems depending on the flexibility of the bonds of functional groups under high pressure.

In this chapter, we introduce the concept of triboluminescence (TL) in lanthanide complexes; TL is a mechanoluminescence (ML) property and refers to the luminescence phenomenon observed when crystals are fractured. Mechanochromic luminescence has been reported in polymorphic systems, and ML could be observed in not only inorganic compounds but also organic crystals and complexes [9–13]. ML systems can be roughly classified into two groups: systems that show photoluminescence (PL) changes under UV excitation and those that show PL without the need for photoexcitation. In this chapter, we focus on the TL of lanthanide complexes, which manifests as luminescence during crystal fracturing under a driving force, such as a shock wave or shearing (Fig. 7.1).

TL can be observed by crushing sucrose crystals or striking quartz rocks against each other with force [14]. While it is a phenomenon that is widely observed in both organic or inorganic compounds, the TL phenomenon is incompletely understood. This problem is attributed to three main reasons: (1) the principle behind TL remains a matter of speculation, (2) the stimulus cannot be quantified at the time of collision, and (3) the available methods and means to observe luminescence and structural phase transitions are insufficient.

Xu et al. [15] observed TL in systems in which Eu and Dy were loaded on Sr alumina. This phenomenon was thus believed to be related to thermally excited states via the defect levels of the alumina. Several hypotheses have been offered to explain the principle of TL in organic molecules and complexes. For example, the excitation of atmospheric N_2 is believed to be promoted by the frictional energy during rubbing, which results in emission [16]. A recent report indicated that X-rays are generated when Scotch tape is rubbed at high speed [17]. Knowledge of the activation principle, manipulation, and material design of the TL phenomenon can lead to the development of new energy-conversion materials.

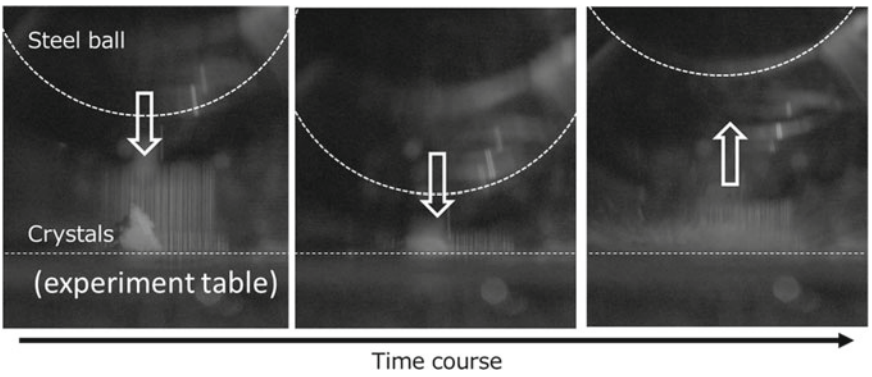

Fig. 7.1 Snapshots of Eu-complex crystals crushed by a drop-tower system and recorded by a high-speed camera (Photoron Co., Ltd.). The ball size diameter is ca. 170 mm (Private data: M. Hasegawa, AGU). See also Fig. 7.8

PL is enhanced or quenched under different atmospheres, such as N_2 or O_2, because the spin multiplicity of orbitals involved in energy relaxation varies depending on the central metal species. In particular, lanthanide complexes are suitable candidates for understanding the photophysical principle of TL because their PL phenomena are based on lanthanide-specific f–f transitions arising from the spin multiplicity of excited organic ligands.

7.2 Aim of This Chapter

In this chapter, we discuss the history and measurement methods of TL, the quantification of stimuli, and various theories of the principle of TL expression, focusing on lanthanide complexes as examples of TL soft crystals. The f-electron configurations of lanthanides are $[Xe]4f^{n+1}$ ($n = 3, 5, 6, 9, 12, 13$; Ln = Nd, Sm, Eu, Dy, Tm, Yb) and $[Xe]4f^n$ 5d ($n = 0, 1, 2, 7, 8, 10, 11, 14$; Ln = La, Ce, Pr, Gd, Tb, Ho, Er, Lu). The luminescence bands can be classified into two main types: f–f transitions localized in f orbitals, which are inherently forbidden, and d–f transitions [18]. In this chapter, we mainly discuss the f–f transitions (or f–f luminescence) of lanthanide complexes with organic molecular ligands.

In general, the PL of lanthanide complexes is due to the highly efficient photoexcitation of π-electronic ligands under UV light irradiation. Energy transfer from the excited ligand to the lanthanide ion promotes f–f luminescence from the latter [19]. In the 1960s, the crystal-field splitting levels of the f orbitals of a series of trivalent lanthanide ions were attributed to the photoemission spectra of He (see Sect. 7.4.1 [20]). The crystal-field splitting levels are not drastically influenced by the surrounding media. Eu^{III} and Tb^{III} show red and green emissions, respectively, when energy transfer is established, regardless of the ligand type. As the absorption coefficient of the f–f transition is very small and the Stokes shift is almost zero, the luminescence obtained from the direct excitation of f–f absorption has weak efficiency. The emergence of f–f luminescence observed via the photoexcitation of the ligand is called the photo-antenna effect, which is used to increase in the efficiency of PL. The luminescence lifetime and quantum yield of PL have been experimentally evaluated in both organic and inorganic luminescent materials.

In contrast to PL, not much about the principle of TL and its possible manifestation is known. The earliest surviving document on this topic dates back 400 years (see Sect. 7.3, [21]). However, the methods for TL evaluation remain in the developmental stage, and various TL molecular designs and principles have been proposed.

Here, we introduce some methods to measure the TL of lanthanide complexes and discuss the effects of soft-crystalline structural changes on this phenomenon.

7.3 History of Triboluminescence Derived from Weak Stimuli

A fundamental issue in chemistry is the relationship between the effects of macroscopic mechanical stress on bulk materials and the molecular-level changes in the structure and properties of these materials [22]. Various mechanochemical effects have been studied to determine this relationship, among which stress and macroscopic distortion were observed to induce changes in microscopic properties, such as mechanochromic, piezoelectric, and photomechanical properties [23]. TL is also an interesting phenomenon of mechanical stress [24]. In the seventeenth century, Francis Bacon observed light emission from sugar cubes during crushing [24]. Different types of materials exhibiting TL, such as organic crystals, polymers, and metal complexes, have been studied [25–27]. The origin of TL has been discussed, and some recent studies have demonstrated the contribution of the piezoelectric effect to this phenomenon during the breakage of non-centrosymmetric bulk crystals [27]. The structure of sugar crystals, which are chiral and, thus, have a non-centrosymmetric structure, is expected to contribute significantly to their obvious TL [28]. The hydrogen-bonding networks in sugar crystals also seem to contribute to their relatively large resistivity against mechanical stress prior to their breakdown and, thus, their intense TL.

The publication trend of studies on TL was determined using the information retrieval system Web of Science (research date: January 20, 2022). The trend of publications on TL and ML is shown in Fig. 7.2.

TL can be induced by crushing the crystals of minerals, sugars, etc. In 1903, Armstrong and Lowry speculated that a two-state transformation based on the structural change of N atoms is induced when crystals of saccharine, a type of sugar, are crushed [29]. In 1910, Andrews reported that yellow TL was produced by crushing a mixture of 70% zinc carbonate, 30% fluorinated sulfur, and a small amount of manganese sulfide [30]. In 1911, Alfred described the TL of U metal in the scientific journal *Nature* [31]. Publications on TL research began to increase in 1967, but only a

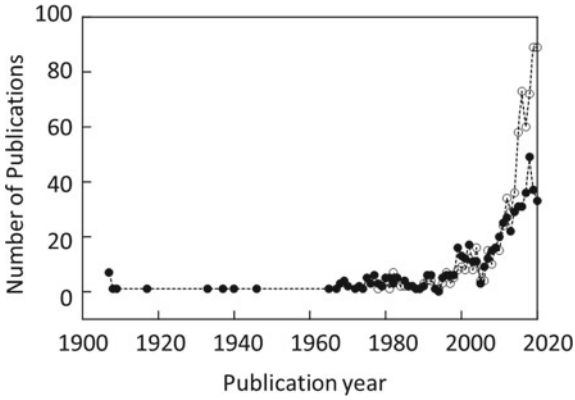

Fig. 7.2 Number of publications on triboluminescence (black dot) and mechanoluminescence (circle) from 1900 to January 2021 in Web of Science®

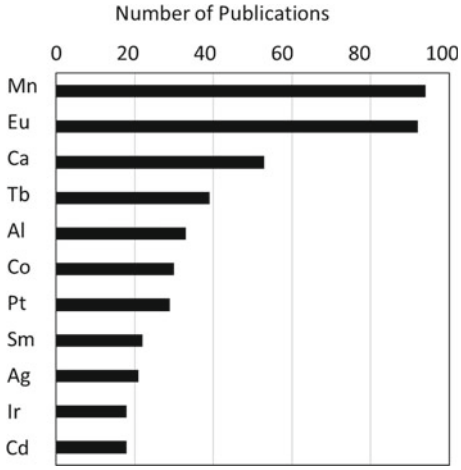

Fig. 7.3 Element-classified statistics of published papers on triboluminescence

few papers on the origins of TL were published annually until the year 2000. Reports on ML began to be increase in 1980. In 2010, the number of papers describing TL and ML were almost equal. In 2020, the number of papers describing ML was four times greater than that describing TL.

Various TL materials and their luminescence phenomena have been reported and investigated worldwide. Figure 7.3 shows the statistics of published papers on TL according to element.

The data show that many reports on TL materials containing Mn and Eu have been published. The TL of both inorganic manganese-compounds and Mn(II) complexes has been reported. The TL of inorganic Eu(II)-ion containing compounds and Eu(III) complexes has also been described. Ca and Al have been reported to be host media for TL materials. TL materials containing Pt and Ir have also been reported.

7.4 Luminescent Lanthanide Complexes

7.4.1 Evaluation of Photoluminescence by the Photo-Antenna Effect

PL provides a large amount of information that could be used to evaluate the TL of lanthanide complexes. Because the experimental method of photoexcitation has previously been established and the apparatus is commercially available, the measurement of PL is relatively easy. Such measurements allow us to determine the position of the luminescence band and quantitatively determine the luminescence lifetime and quantum yield. Here, we describe the principle of the PL of lanthanides and its evaluation.

The f–f transition of lanthanide ions involves a transition between electronic levels due to the splitting of the f orbital. This level is not susceptible to the so-called ligand field, unlike d-group metal ions, because lanthanides are inner-shell transition-metal ions, and the f orbital, which controls the properties, is in the inner shell, while the d or s orbitals, which are involved in bonding, are in the outer shell. Given this electronic structure, the half-width of the absorption or emission band due to the f–f transition is narrower and less affected by the coordination field compared with those of d-meal complexes. In other words, the splitting energy levels of the f orbitals are constant for any coordination atom or ligand, which can be attributed to a series of He photoemission spectra of lanthanide chlorides [20]. A diagram of these energy levels is called a Dieke diagram (Fig. 7.4).

Because f–f transitions are inherently forbidden and the Stokes shift is small, deriving the f–f emission from the excitation of the absorption bands of f–f transitions is challenging. The optical antenna effect can overcome this difficulty. The photo-antenna effect can enhance the f–f emission of lanthanide ions via the excitation energy of a π-electronic ligand with a large absorption coefficient complexed with a lanthanide ion [33].

In general, many complexes of Eu and Tb have been synthesized because they show red and green luminescence, respectively. Establishing a good relationship between the excited state energy of the ligand and acceptor level of Eu and Tb is important for more efficient luminescence. The concepts of Dexter- [34] or Förster [35]-type energy transfer can be applied to the optical antenna effect of lanthanide complexes, which is based on (1) energy level resonance between the energy donor (EnD) and acceptor (EnA), (2) energy transfer between the EnD and conservation of spin multiplicity before and after energy transfer at the EnA level, and (3) the distance between the EnD and EnA (Fig. 7.5).

The Dieke diagram (Fig. 7.4) shows that the EnA level depends on the type of metal ion. Therefore, the EnD level can be designed as necessary to promote highly efficient energy transfer and luminescence. In fact, the singlet energy level of Pr functions as EnA and a molecule tailored to this level can promote f–f luminescence at the selected level [32]. The EnD levels of the ligands of lanthanide complexes can be determined by coordinating them with Gd, which does not have an EnA level, and measuring its fluorescence and phosphorescence to determine the position of the excited singlet and triplet, respectively [36].

7.4.2 Evaluation Methods of Triboluminescence

TL could be manifested by directly applying mechanical stimuli, such as pressure [37], rubbing [38], laser ablation [39], and direct impact [40], to crystals, for example, by (Fig. 7.6). Video recording followed by image analysis and spectral detection by connecting optical fibers to a small spectrometer, for instance, have been reported. Quantifying stimuli and quantitative TL analysis are still under development. In this section, we introduce the evaluation methods of TL materials.

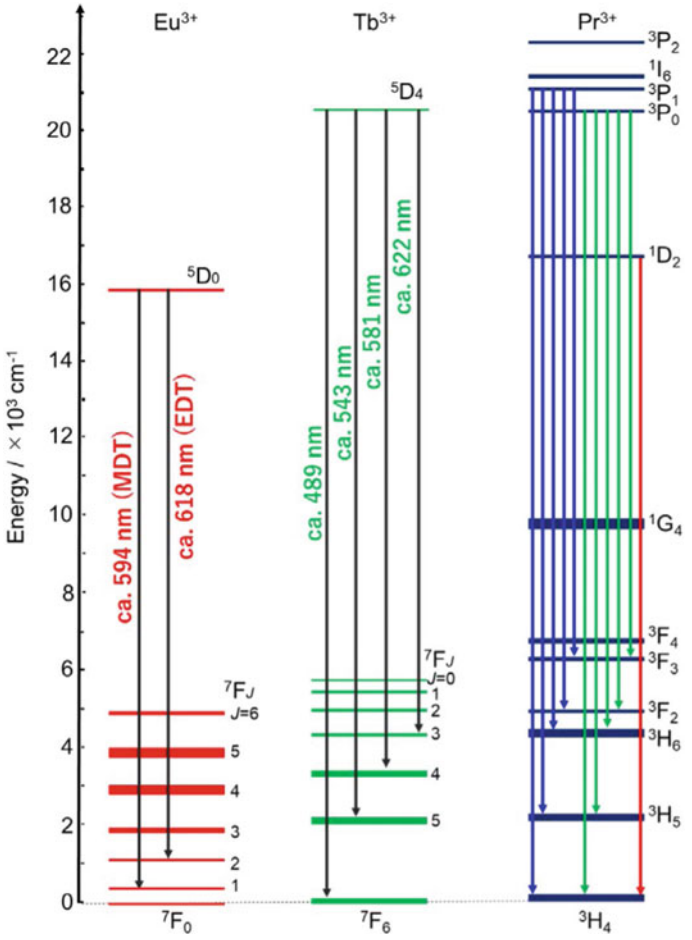

Fig. 7.4 Dieke diagram of trivalent Eu, Tb, and Pr ions for different luminescence band wavelengths. MDT = magnetic dipole transition; EDT = electric dipole transition. Ref. [32] Copyright (2020) Chemical Society of Japan

Many reports of the use of digital cameras to capture the exact moment when crystals are crushed or rubbed with a metal spatula or glass rod have been published [41]. Such recordings are important to the observation of TL in the visible region.

Xu et al. developed a method in which an inorganic oxide exhibiting mechanical luminescence is mixed with a polymer and solidified into a disc; the disc is then stimulated by rubbing at different rotational speeds [38].

Xu et al. combined the method of constant pressure and observation in a photo cell to measure the spatial distribution of luminescence in situ (Fig. 7.7) [37]. They also reported a method in which a sample is applied to a stainless-steel plate with crack-inducing slits and the plate is pulled at opposite sides to observe the resulting

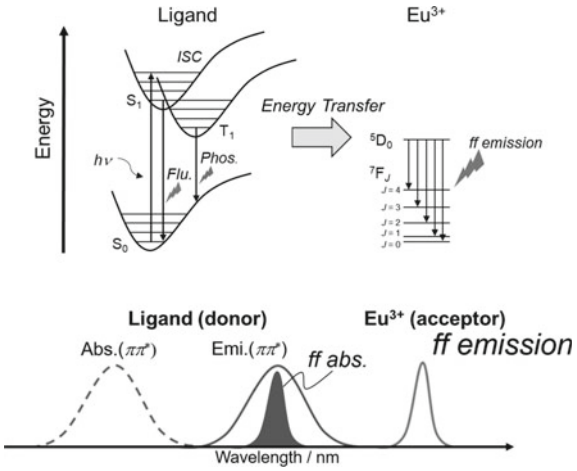

Fig. 7.5 Energy diagram of the f–f emissions induced by the photo-antenna effect (top). Principle of the acceleration of energy transfer by the superimposition of ligand-centered emission (π–π* transition) and lanthanide-centered absorption (f–f transition) (bottom)

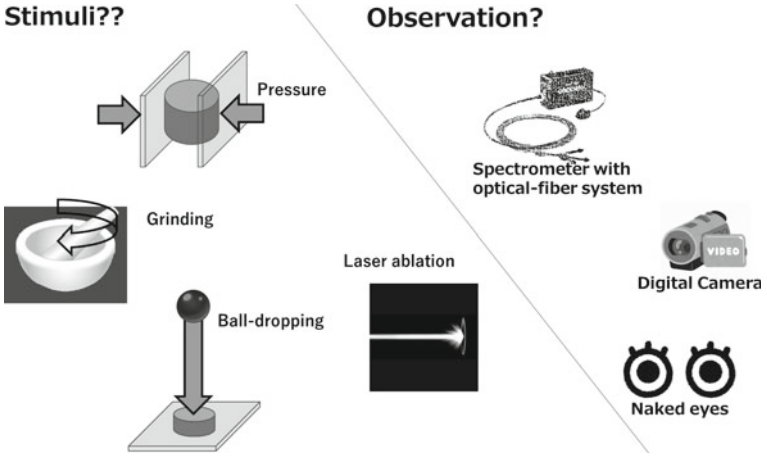

Fig. 7.6 Various stimuli used to enhance triboluminescence and its observation methods

TL. This approach could be used as a diagnostic method to visualize the correlation between cracks in the stainless-steel plate and the distorted portions of the plate, not just single crystals.

Tsuboi et al. reported the quantitative measurement of the TL of sucrose using laser ablation [39]. Suslick et al. successfully induced TL with ultrasound and measured its spectrum [39]. Ilatovskii et al. reported a method to achieve the quantitative stimulation of membraned TL materials using a texturometer [39].

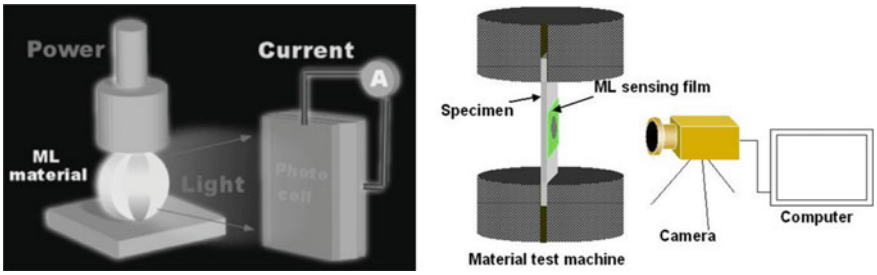

Fig. 7.7 Image of the mechano-luminescence sensing system. Ref. [37] Copyright (2007) The Japan Society of Applied Physics and (2008) The Visualization Society of Japan, respectively

Fontenot et al. [40] and İncel et al. [41] related the free-dropping energy of a metal ball dropped from various heights to the TL intensity (Fig. 7.8). Based on this system, M. Hasegawa et al. developed a drop-tower system (DTS) that used a pipe made of methyl polymethacrylate, attached a starter at an arbitrary height, and freely dropped a stainless-steel ball [42]. The edge of the optical fiber was attached to a plate, which served as a falling point, and TL was observed through the polycarbonate plate; the wavelength and relative emission intensity of this luminescence were then recorded by a small spectrometer. Placing the entire device in a glove bag allowed for the measurement of TL spectra in atmospheres of Ar and N_2. In addition, the potential energy due to free fall can be estimated from the height and the mass of the stainless-steel ball.

Sage et al. developed a detection method for measuring the TL of a series of organic crystals [43]. Longchambon et al. devised another measurement method in which the crystals were entrained in an airstream and impinged on a quartz substrate placed in front of a detector (Fig. 7.9) [44]. Unfortunately, this method was not suitable for fine particles. Meyer et al. applied the leverage principle and reported an impact method in which a needle was dropped onto a crystal [45]. In this system,

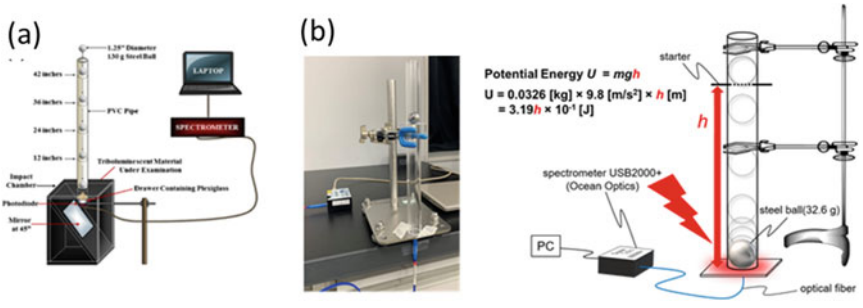

Fig. 7.8 Drop-tower system developed by İncel et al. (**a**) and its modified version using a transparent tube (**b**). Refs. [41, 42] Copyright (2017) American Chemical Society, and (2020) The Imaging Society of Japan

changing the number of weights allowed for variations in the magnitude of the impact, and the apparatus itself could be placed in a box to allow experiments in different environments. Nowak et al. developed an apparatus in which a crystal was placed between a gear and plate and the force of the gear turning with the weights crushed the crystal [46]. Based on these trial-and-error methods, the methods of crushing by a piston using compressed air (Fig. 7.10) [47], placing a crystal on a detector and impacting it with a plastic plug in free fall [48], and suspending a weight on a pulley and letting it fall freely [49] were also devised.

Hasegawa et al. evaluated the TL performance of pulverized crystals under magnetic stirring in an atmosphere-controlled flask by detecting the resulting TL spectrum and analyzing the images captured by a charge-coupled device (CCD) camera (Fig. 7.11). Using this method, the authors found that the polymer chain arrangement of Eu(III) coordination polymers in the crystals affected their TL intensity [50].

Time-dependent TL multiplied by an instantaneous impact has been reported. Hasegawa et al. analyzed the emission lifetime of Eu(III) coordination polymers using a nanosecond pulsed laser (Fig. 7.12) [51]. The TL emission spectra and emission lifetime analyses of 4f–4f transitions in this Eu(III) coordination polymer indicated that the nonradiative rate in the TL process is approximately five times higher

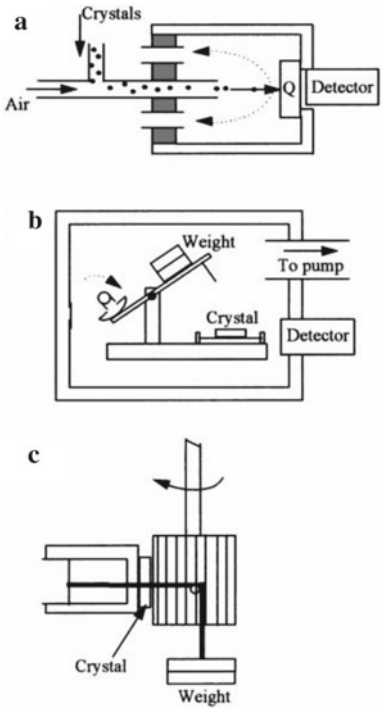

Fig. 7.9 Methods for inducing triboluminescence. **a** The air-driven technique, **b** the impacting-needle technique, and **c** the crystal-milling technique. Ref. [43] Copyright (2001) Royal Society of Chemistry

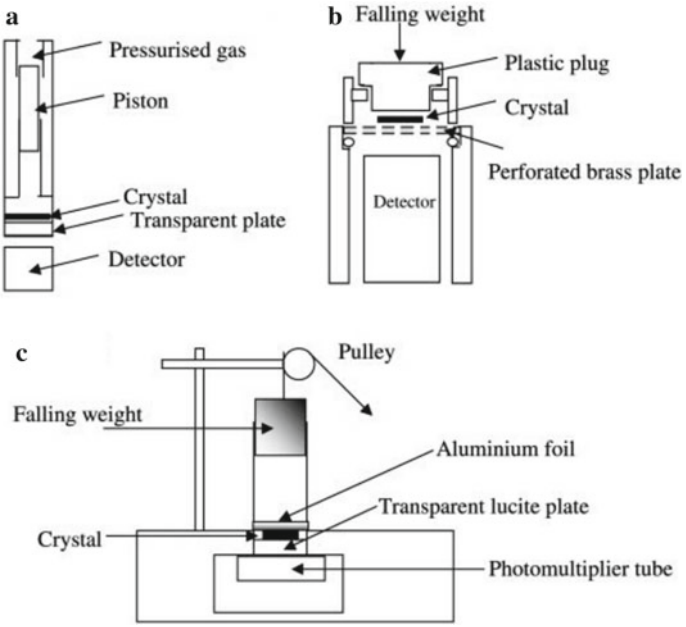

Fig. 7.10 Modern techniques for inducing triboluminescence. **a** The air-driven piston technique, **b** the falling-weight technique, and **c** a variant of the falling-weight technique. Ref. [47] Copyright (1980) American Physical Society

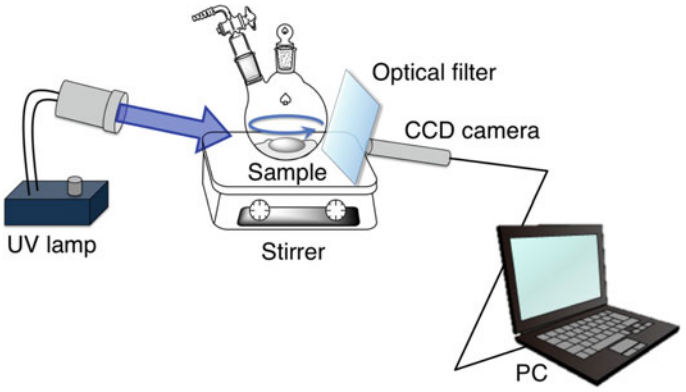

Fig. 7.11 Method for triboluminescence observation. Magnetic stirring is conducted in an atmosphere-controlled flask, the resulting spectrum is detected, and the images captured using a CCD camera are analyzed. Ref. [50] Copyright (2017) Wiley–VCH Verlag GmbH & Co. KGaA, Weinheim

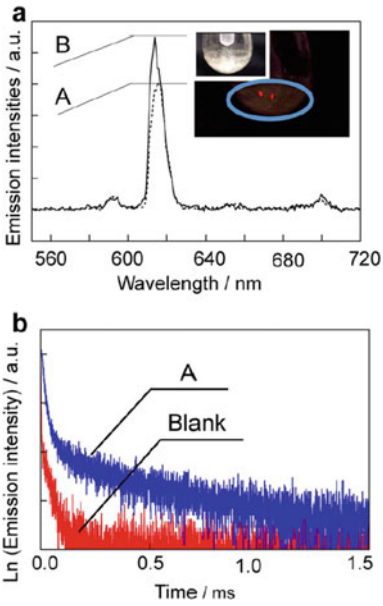

Fig. 7.12 **a** Triboluminescence (TL; A:a) and photoluminescence (PL; B:c) spectra. The PL spectrum is observed by excitation at 355 nm. Inset: TL image of $[Eu_3(hfa)_9(tppb)_2]_n$. **b** Emission decay profiles of the TL of $[Eu_3(hfa)_9(tppb)_2]_n$ (A: blue line) and $BaSO_4$ powders (blank: red line) under shockwave irradiation. Ref. [51]. Copyright (2017) Wiley–VCH Verlag GmbH & Co. KGaA, Weinheim

than that in the photo-excited luminescence process. In other words, TL involves a larger nonradiative process compared with photoexcited luminescence.

Time-resolved TL analysis has been performed using shock waves in which the air pressure can be controlled (Fig. 7.13) [52]. In this system, the TL of Tb(III) and Eu(III) coordination polymers was measured under air shock wave (ASW) pressures ranging from 100 to 400 kPa. The photophysical data obtained from the time-resolved TL analysis indicated that the TL intensity of the Tb(III) coordination polymer depended on the air pressure, which was related to the energy transfer process (Fig. 7.13). Thermal effects on TL were hardly observed under the experimental conditions employed, but oxygen pressure affected the TL performance. TL experiments using Tb(III)/Eu(III) mixed coordination polymers demonstrated that the energy transfer process from Tb(III) to Eu(III) is not as effective as the photoexcitation process (Fig. 7.14).

7.4.3 Discrete Complex Systems with Lanthanide Ions

In this section, we describe the TL phenomena and molecular structures and arrangements of lanthanide complexes, in which discrete molecules are packed into a crystal lattice. Various combinations of molecular structures and compositions have been reported to control the conditions for TL manifestation. For example, a series of tetrakis(β-diketonate)Ln derivatives have been used to discuss the symmetry of crystal systems [53–55]. Chandra et al. [53] reported that they produced TL only

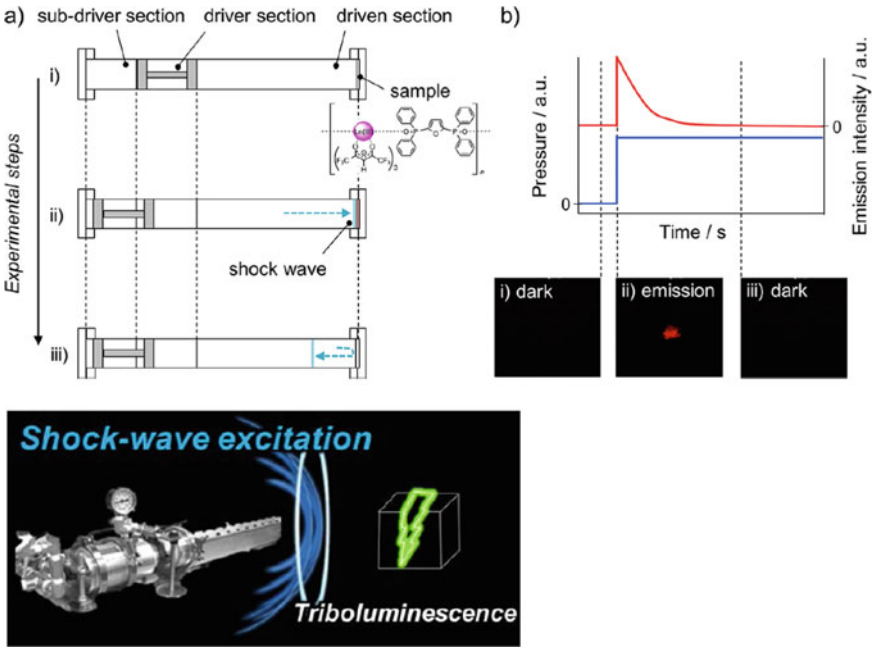

Fig. 7.13 **a** Schematic of aerodynamic shock wave experiments and **b** the corresponding profiles and images (red line, emission profile; blue line, pressure profile). Ref. [52]. Copyright (2019) American Chemical Society

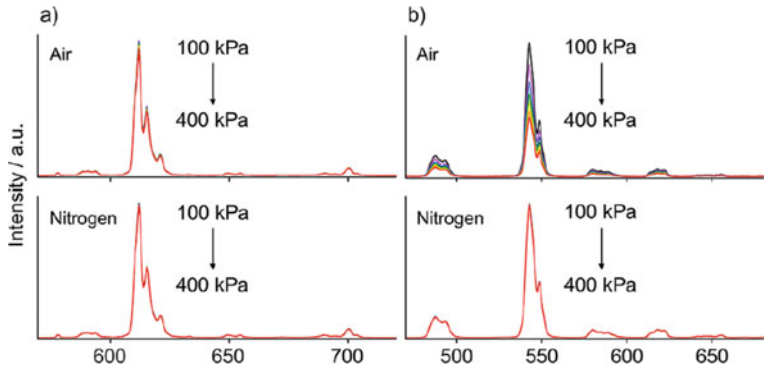

Fig. 7.14 Pressure-dependent emission spectra of **a** $[Eu(hfa)_3(dpf)]_n$ and **b** $[Tb(hfa)_3(dpf)]_n$ under air and N_2 gas ($\lambda_{ex} = 380$ nm, P = 100–400 kPa, solid state). Ref. [52]. Copyright (2019) American Chemical Society

in pyroelectric crystals with non-centrosymmetric symmetry. By contrast, Cotton [54] and Wong [56] found that TL also occurs in crystalline systems with central symmetry. The relationship between central symmetry and TL has been discussed for ternary complexes of Eu and Tb with bipyridine or 1,10-phenanthroline coordinated to tetrakis(β-diketonate)Ln; the findings of some related studies are summarized in Fig. 7.15 and Table 7.1 [26, 56–59].

The compound $(dbm)_3bpy$ shows TL even as centrosymmetric crystals, while the non-centrosymmetric crystal $Eu(dbm)_4TMP$ is pyroelectric and shows strong TL properties under pressure (Fig. 7.16) [56]. Similar considerations have been reported

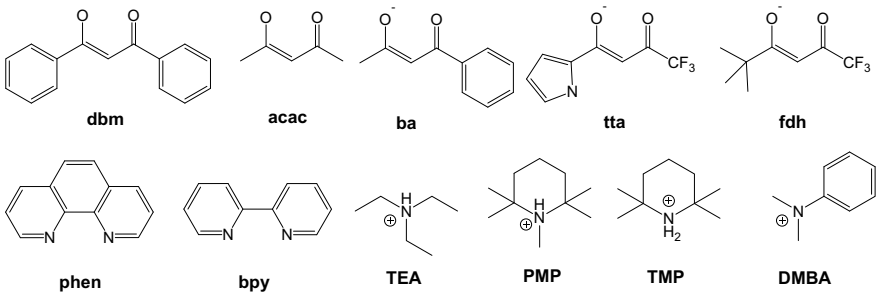

Fig. 7.15 Examples of organic ligands to induce TL of lanthanide in their complexes

Table 7.1 Summary of the TL activities and crystal structural properties of Ln(III) complexes

Compound	TL activity	Space group	Crystal symmetry	References
$Eu(dbm)_3phen$	**Inactive**	**P21/c**	**Centrosymmetric**	[56]
$Eu(dbm)_3bpy$	**Active**	**P-1**	**Centrosymmetric**	[56]
$Eu(tta)_3phen$	**Active**	**$Pca2_1$**	**Non-centrosymmetric**	[56]
$Eu(tta)_3bpy$	**Active**	**$P2_1/n$**	**Centrosymmetric**	[56]
$Eu(fdh)_3phen$	**Inactive**	**$P4_12_12$**	**Non-centrosymmetric**	[56]
$Eu(fdh)_3bpy$	**Active**	**P-1**	**Centrosymmetric**	[56]
$Eu(dbm)_4TEA$	**Active**	***Cc***	**Non-centrosymmetric**	[56]
$Eu(dbm)_4PMP$	**Inactive**	**P-1**	**Centrosymmetric**	[56]
$Eu(dbm)_4TMP$	**Active**	**Pca21**	**Non-centrosymmetric**	[56]
$Eu(tta)_3PMP$	**Active**	**$P\text{-}42_1c$**	**Non-centrosymmetric**	[56]
$Eu(tta)_3TMP$	**Active**	**$P\text{-}42_1c$**	**Non-centrosymmetric**	[56]
$Eu(dbm)_4TEA$	**Active**	***I 2/a***	**Centrosymmetric**	[26]
$Eu(dbm)_4DCM$	**Inactive**	***I 2/a***	**Centrosymmetric**	[26]
$Tb(ba)_4PP$	**Active**	**$P2_1/n$**	**Centrosymmetric**	[26]
$Eu(dbm)_4DMBA$	**Active**	**$Pca2_1$**	**Non-centrosymmetric**	[60]
$Tb(acac)(phen)_2$	**Active**	***P2/n***	**Centrosymmetric**	[61]
$Tb(acac)_3phen$	**Active**	**$P2_1/n$**	**Centrosymmetric**	[58]

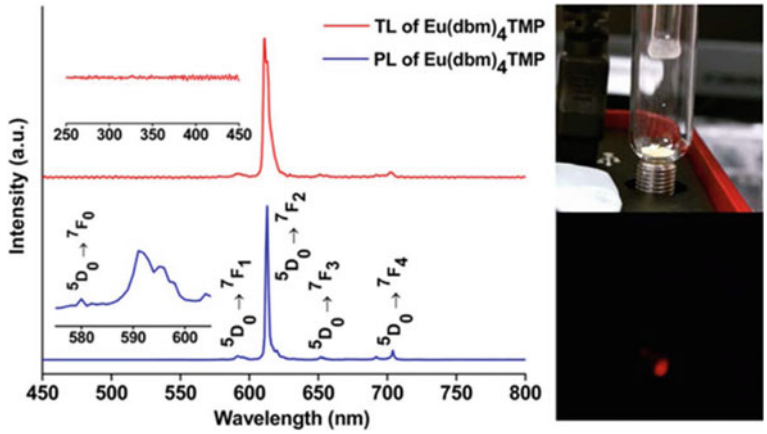

Fig. 7.16 TL and solid-state PL spectra of Eu(dbm)$_4$TMP at room temperature. The images on the right show the CCD spectrometer captureing light emission induced by fracture of the crystals. Ref. [62] Copyright (2004) Elsevier B. V

for other systems [57–61, 63, 64]. Sweeting et al. found that triethylammonium tetrakis(benzoylethanate)Eu exhibited TL when recrystallized in methanol but not in dichloromethane (DCM) (Fig. 7.17) [26]. The former involves TEA coordination to the Eu ion and the latter involves a solvent for crystallization [5]. Li et al. observed TL and dielectric properties from the polymorphs of Eu complexes of tetrakis(β-diketonate)Ln coordinated with a terpyridyl derivative with chiral moieties [57]. They experimentally showed that crystals in the space group $P2_1$ (monoclinic) exhibited a TL band that could be attributed to the f–f transition of Eu ($^5D_0 \rightarrow {}^7F_2$) as well as good dielectric properties. By contrast, the polymorphic crystals of space group $P2_12_12_1$ (orthorombic) showed no TL or dielectric properties. These results indicate that TL depends on the polarity of the crystals (Fig. 7.18).

The research groups of Kalinovskaya and Bukvetskii used a ternary complex with quinalidic acid mixed with Eu/Tb(acac)$_4$ or phen as a matrix and argued that the piezoelectric effect affects the TL expression of this complex (Fig. 7.19) [58, 59, 61, 63]. Crystal structural analysis showed the formation of a layered structure and importance of the concepts of “destruction zone” and “destruction zone width” due to mechanical impact to TL expression. Based on a similar consideration of the crystal system, Bukavetskii et al. reported the TL expression of Sm complexes [59].

Structural or chemical driving forces, for example, charge separation during crystal fracturing and dielectric properties, are believed to be involved in the manifestation of TL upon stimulation. However, owing to the difficulty of instantaneous measurement, whether this belief is accurate remains a matter of speculation (Figs. 7.19 and 7.20) [65]. Hasegawa et al. recently applied nitric acid as a reductive counter anion and performed TL experiments using a DTS on the chiral crystals of lanthanide complexes with amino acid derivated-bipyridine derivative (Fig. 7.21) [37]. This complex also forms racemic crystals [66], but they did not

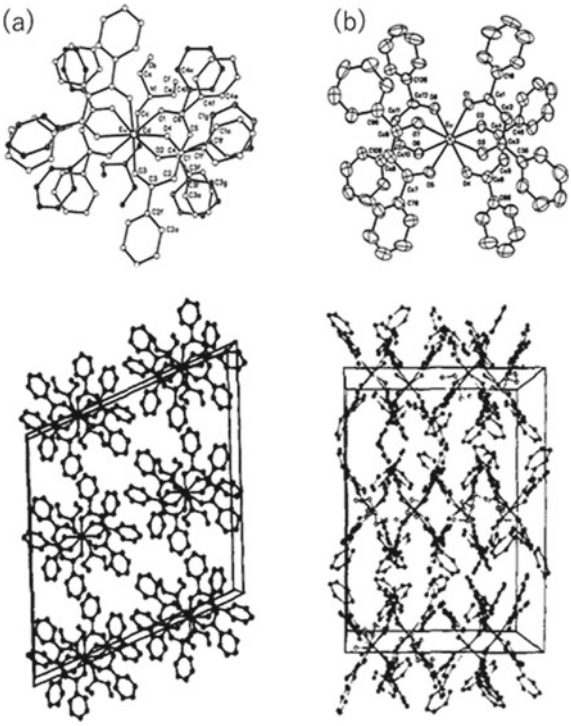

Fig. 7.17 Molecular structures and unit cell packing diagrams for **a** triboluminescent Eu complex and **b** non-triboluminescent one containing solvent of crystallization. Ref. [26] Copyright (1987) American Chemical Society

show TL. This finding suggests the possibility of a system associated with chemical reactions. Kubota and Ito et al. suggested that the presence of electrons is useful in promoting coupling reactions with hammering stimuli [65]. Such findings indicate a novel mechanism for the driving force of TL.

7.4.4 Coordination Polymer Complexes

Coordination polymers composed of metal complexes and organic ligands have been studied extensively in recent years. One-, two-, and three-dimensional organic–inorganic hybrid polymers have been reported. In 2004, Yuan reported the TL phenomenon of $[Eu(TPA)_3(HTPA)_2]_n$ (TPA: α-thiophene carboxylate, HTPA: α-thiophenecarboxylic acid) without emission spectra (Fig. 7.22) [67]. Eliseeva described the TL spectra of red-luminescent Eu(III) ($[Eu(hfa)_3(dmtph)]_n$ and green luminescent Tb(III) $[Eu(hfa)_3(dmtph))]_n$ (dmtph: 1,4-dimethyltherephtalate) coordination polymers for the first time (Fig. 7.23). [62] In 2011, Hasegawa reported the TL phenomenon of $[Eu(hfa)_3(bipypo)]_n$ (bipypo: 3,3-bis(diphenylphosphoryl)-2,2-bipyridine) with a high emission quantum efficiency (71% at 465 nm excitation) (Fig. 7.24) [68]. Hasegawa also reported the ratiometric TL spectra and

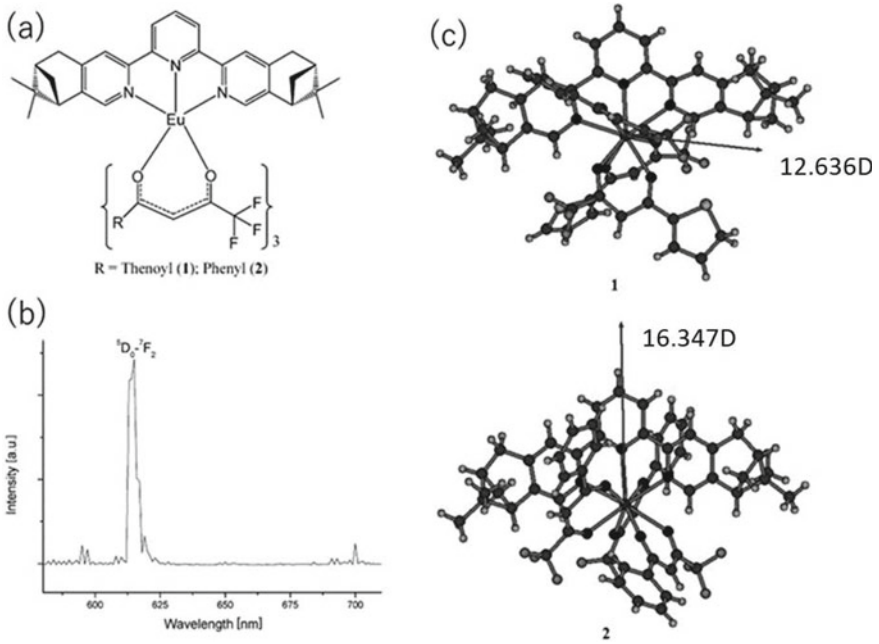

Fig. 7.18 Chiral terpyridyl Eu Complex (**a**), triboluminescence spectrum of the complex (**b**) and the dipolemoments of TL active (1) /inactive (**b**) species (**c**). Ref. [57] Copyright (2009) Wiley–VCH Verlag GmbH & Co. KGaA, Weinheim

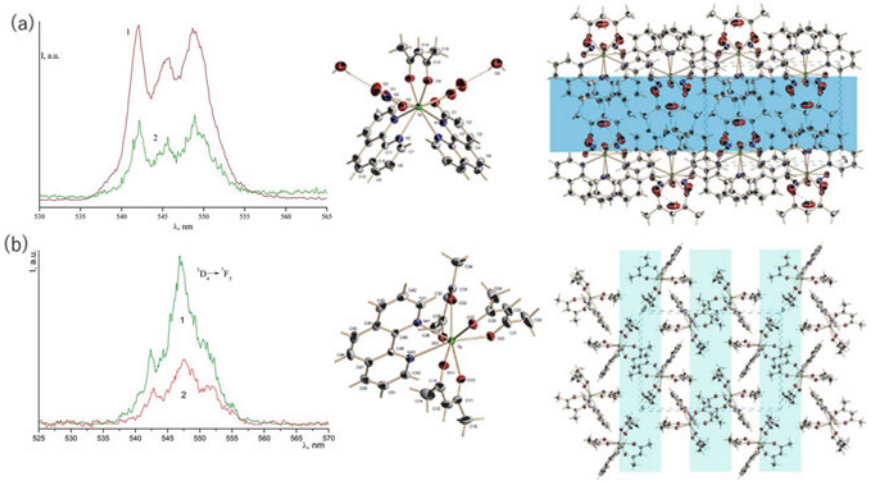

Fig. 7.19 TL (red) and PL (green) spectra and observed molecular structure and packings of $Tb(NO_3)(acac)(phen)_2$ (**a**) and $Tb(acac)_3phen$ (**b**). Refs. [58, 61] Copyright (2016) John Wiley & Sons, Ltd. and (2018) Elsevier B. V

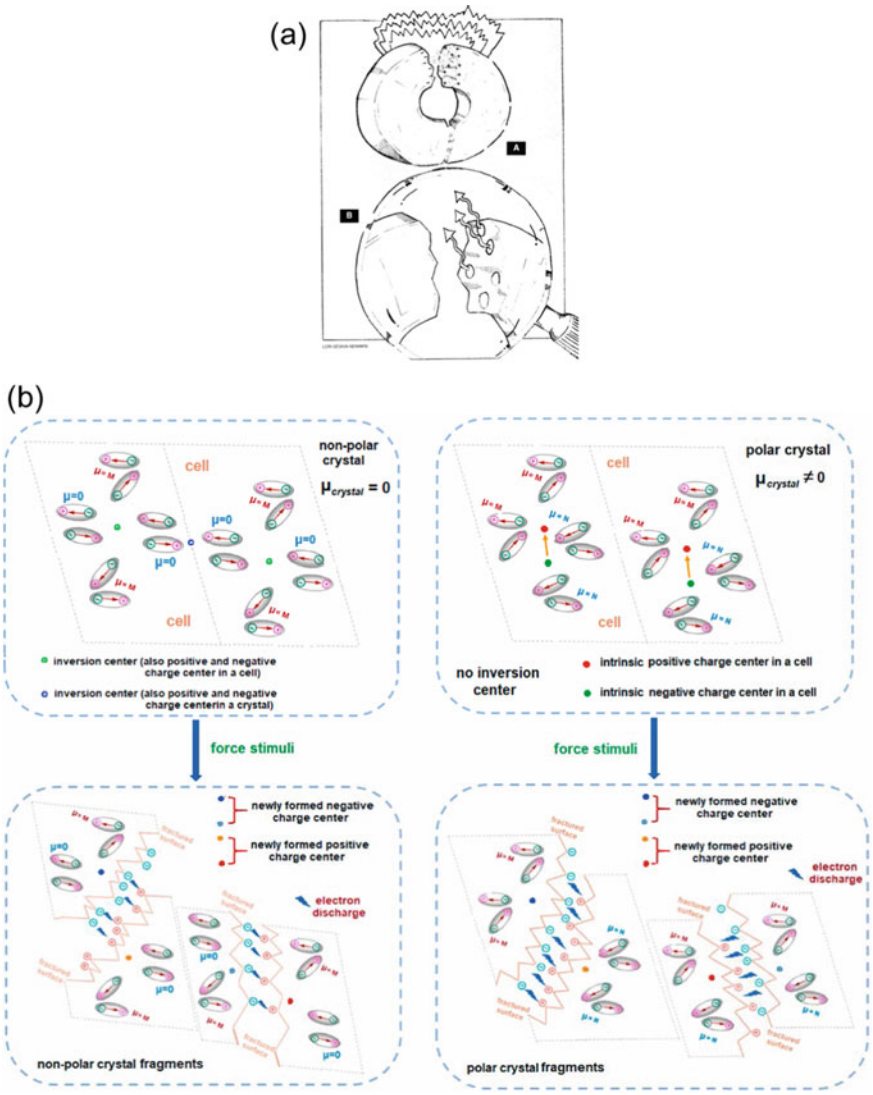

Fig. 7.20 **a** When a candy is cracked open resulting the TL. **b** Schematic diagrams of mechanoluminescence on crystals with non-and centrosymmetric space group. Ref. [64] Copyright (1990) American Chemical Society and (2020) Elsevier Ltd, respectively

images of mixed green- and red-luminescent Eu(III)/Tb(III) coordination polymers $[Eu,Tb(hfa)_3(dpt)]_n$ (dpt: 2,5-bis(diphenylphosphoryl)thiophene). The spectral intensity ratio of the green and red emission bands of the TL of these polymers under crystal milling were different from that of their PL (Fig. 7.25) [50, 69]. This difference in spectral intensity ratio is due to population differences

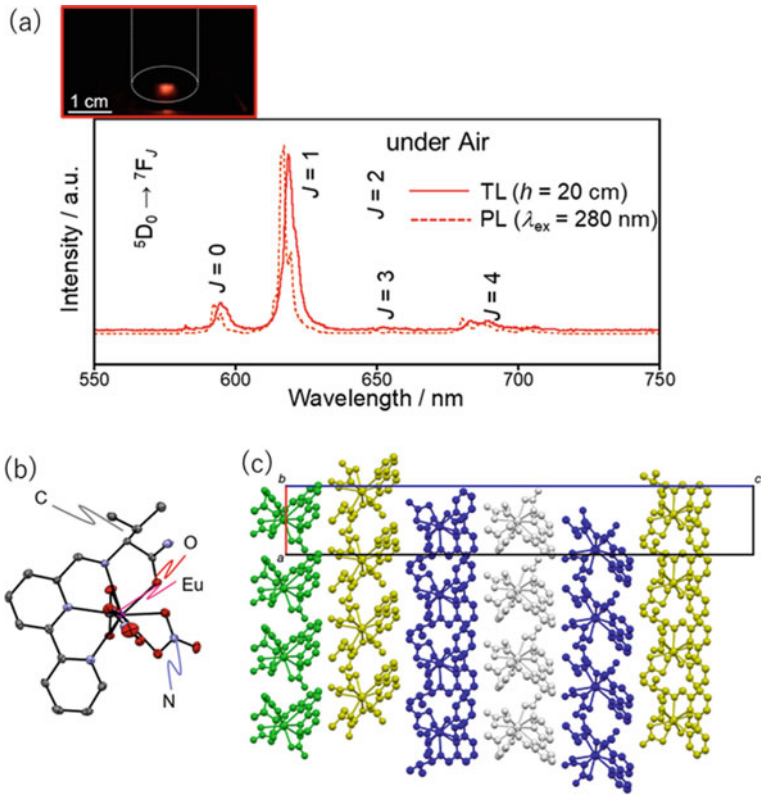

Fig. 7.21 TL of a chiral Eu complex with tetradentate ligand observed by modified dorop-tower system (**a**) and the molecular structure (**b**) and packing (**c**) of the complex

between PL and TL. Analysis of the TL of $[Eu_3(hfa)_9(tppb)_2]_n$ (dppb: tris(4-diphenylphosphorylphenyl)benzene (tppb)) induced by laser shock wave has been performed [51]. This analysis revealed that the radioluminescence-free deactivation rate during the luminescence process is enhanced in TL. The TL analysis of Eu(III) coordination polymers under laser shock wave has also been conducted. [52] Wu reported the TL phenomena of helical Sm(III) and Eu(III) coordination polymers $[Ln_2(L)_3(H_2O)_5]\infty$-$3H_2O$ (L: 2-(2-hydroxy-3,5-dinitrophenyl) (Fig. 7.26) [70]. Photochemical reactions using the TL phenomena of Eu(III) coordination polymers were recently observed (Fig. 7.27) [71].

The TL of Mn coordination polymers has been reported. In 2020, Artem'ev reported that a Mn coordination polymer $[MnX_2(L)]_n$, with phosphine oxide and carborane units showed blue TL (Fig. 7.28) [72]. Although the TL of tetrahedral Mn compounds had been reported in 1961, this report was the first to present a polymeric Mn system with a tetrahedral structure [73].

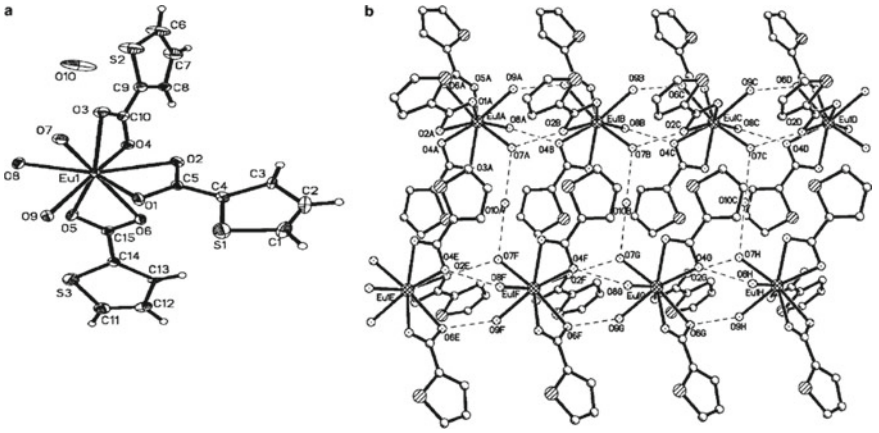

Fig. 7.22 Coordination structures of a) $[Eu(TPA)_3(HTPA)_2]_n$. Ref. [67] copyright (2004) Elsevier B. V

At present, reports on the TL of coordination polymers are scarce. The TL analysis of coordination polymers containing several types of luminescent metal ions will greatly contribute to the understanding of TL phenomena.

7.5 Conclusions

In this chapter, the TL of lanthanide complexes, including its historical background, observation methods, and recent examples of discrete molecular arrangements and coordination polymer systems, were described.

In systems containing lanthanides in oxides and other materials, ML or TL materials based on SrAlO:Dy,Eu [74], which is widely known as a phosphorescent agent, have been the subject of intensive research and are expected to be useful as a diagnostic technology for structures such as bridges [75]. The mechanism of the PL phenomenon of this type of compounds is believed to involve thermoluminescence, which has yet to be reported for lanthanide complexes.

Lanthanide complexes contain significantly fewer lanthanide ions than inorganic ML materials. Moreover, the electronic state unique to lanthanides does not only involve energy conversion, such as PL; the TL phenomenon itself is the visualization of the force. The TL of lanthanide complexes may be related to the thermoluminescence mechanism described above. A system in which lanthanide complexes were mixed with polymers demonstrated a chemical reaction upon stretching, and chemiluminescence was considered the driving force behind this luminescence [76]. Research on the TL of lanthanide complexes remains in its infancy and should be expanded to promote the applications of soft crystals as future energy-conversion devices.

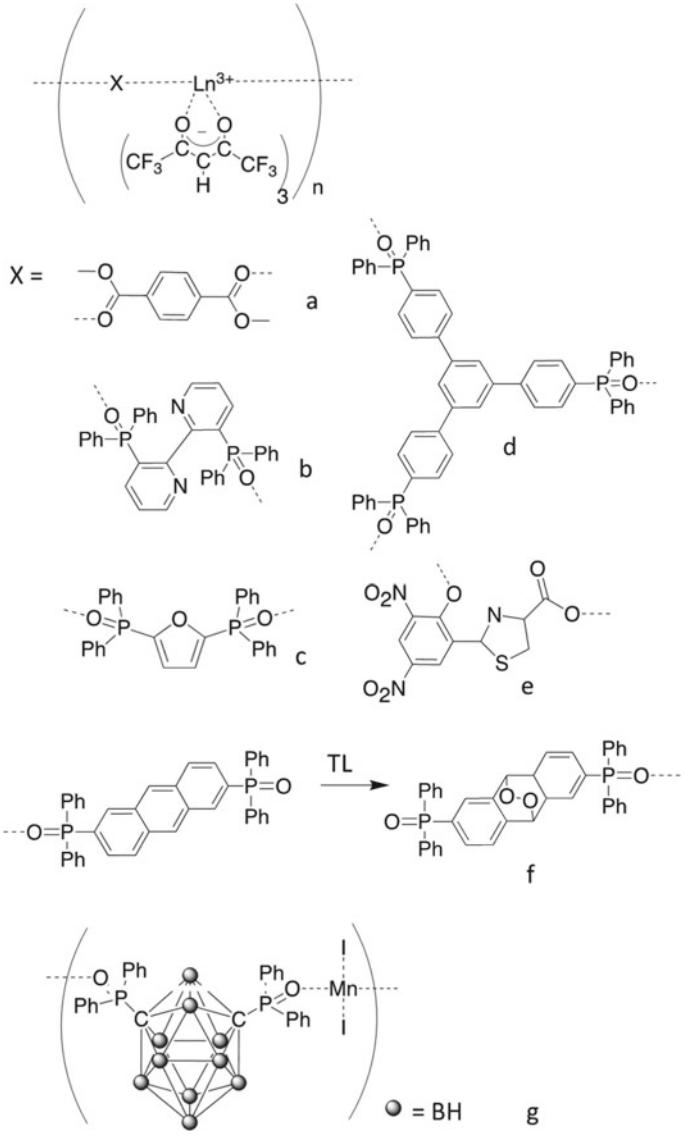

Fig. 7.23 Chemical structures of **a** $[Eu(hfa)_3(dmtph))]_n$ [62], **b** $[Eu(hfa)_3(bipypo)]_n$ [68], **c** $[Eu,Tb(hfa)_3(dpt)]_n$ [51], **d** $[Eu_3(hfa)_9(tppb)_2]_n$ [52], and **e** $[Ln_2(L)_3(H_2O)_5]\infty\text{-}3H_2O$ [70], **f** Photochemical reactions using the TL phenomena of Eu(III) coordination polymers [71], and **g** $[MnX_2(L)]_n$ [72]

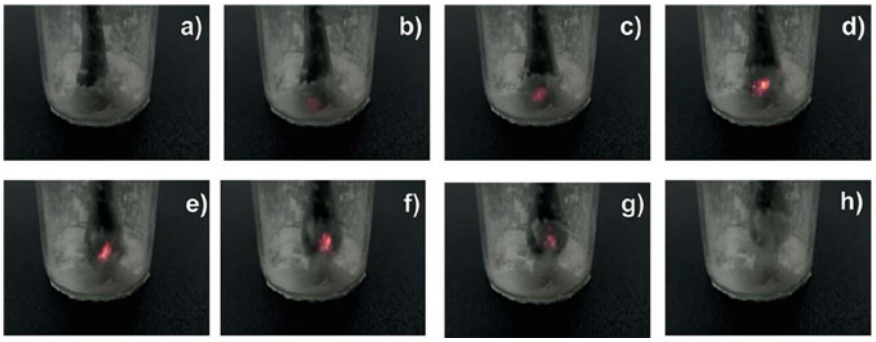

Fig. 7.24 Observed sequence-picture images of triboluminescence $[Eu(hfa)_3(bipypo)]_n$ powder upon pushing with a black stick at ambient temperature and in daylight. Ref. [50]. Copyright (2017) Wiley–VCH Verlag GmbH & Co. KGaA, Weinheim

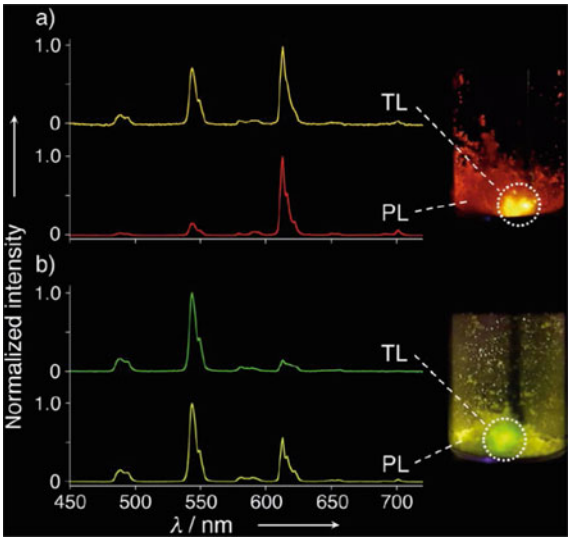

Fig. 7.25 Normalized TL and PL spectra and images of **a** $[Tb,Eu(hfa)_3(dpf)]_n$ (Tb/Eu = 1) and **b** $[Tb,Eu(hfa)_3(dpf)]_n$ (Tb/Eu = 10) Ref. [51]. Copyright (2017) Wiley–VCH Verlag GmbH & Co. KGaA, Weinheim

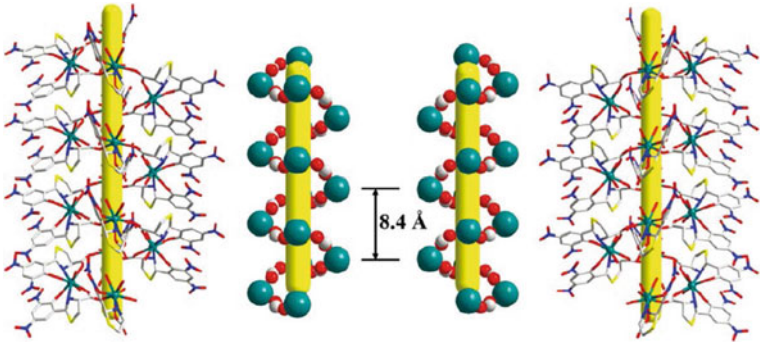

Fig. 7.26 Chiral coordination polymer of Eu complexes with helical structure of Δ-(left) and Λ-form (right). Ref. [70]. Copyright (2022) Royal Society of Chemistry

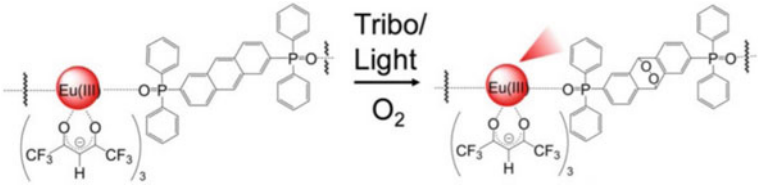

Fig. 7.27 Chemical reaction under the stimuli by tribo or light of the coordination polymer of Eu complexes. Ref. [71]. Copyright (2021) Wiley–VCH Verlag GmbH & Co. KGaA, Weinheim

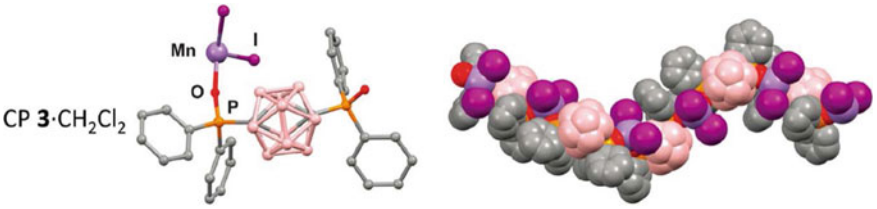

Fig. 7.28 Coordination polymer of Mn complex showing green TL. Ref. [72]. Copyright (2021) Royal Society of Chemistry

References

1. Kato M, Ito H, Hasegawa M, Ishii K (2019) Chem Euro J 25:5105
2. Traylor TG, Luo J, Simon JA, Ford PC (1992) J Am Chem Soc 114:4340
3. Liu H, Dai Y, Wang K, Zhang S, Chen G, Zou B, Yang B (2020) J Am Chem Soc 142:1153
4. Crane DR, Ford PC (1991) J Am Chem Soc 113:8510
5. Tran D, Bourassa JL, Ford PC (1997) Inorg Chem 36:439–442
6. Lechner A, Gliemann G (1989) J Am Chem Soc 111:7969
7. Gu Y, Wang K, Dai Y, Xiao G, Ma Y, Qiao Y, Zou B (2017) J Phys Chem Lett 8:4191
8. Ma Z, Liu Z, Lu S, Feng X, Yang D, Wang K, Xiao G, Zhang L, Redfern SAT, Zou B (2018) Nature Commun 9:4506

9. Bünzli JCG, Wong K-L (2018) J Rare Earths 36:1
10. Nakayama H, Nishida J, Takeda N, Sato H, Yamashita Y (2012) Chem Mater 24:671
11. Nowak R, Krajewska A, Samoć M (1983) Chem Phys Lett 94:270–271
12. Tsuboi Y, Seto T, Kitamura N (2008) J Phys Chem 112:6517
13. Shuang Y, Xie R-J (2021) Adv Mater 33:2205925
14. (a) Zink JI (1978) Acc Chem Res 11:289; (b) ChampmanGN, Walton AJ (1983) J Appl Phys 54:5961; (c) Walton AJ (1997) Adv Phys 26:887
15. Akiyama M, Xu C-N, Nonaka K, Watanabe T (1998) Appl Phys Lett 73:3046
16. (a) Zink JI (1981) Naturwissenschaften 68:507; (b) Sharipov FL, Tukhbatullin AA, Abdrakhmanov AM (2001) Prot Metals Phys Chem Surf 47:13
17. Camara CG et al (2008) Nature 455:1089
18. Bünzli J-CG (2015) Coord Chem Rev 293–294:19
19. Bünzli J-CG (2005) C Piguet 34:1048
20. (a) Dieke GH (1961) Adv Quantum Electron. In: Singer JR (ed). Columbia University Press, New York; (b) Dieke GD, Crosswhite HM (1963) Appl Opt 2:675; (c) Dieke GH, Crosswhite HM, Dunn B (1961) J Opt Soc Am 51:820
21. Bacon FThe advancement of learning, vol 1605. Macmillan, Novem Organum, London, p 209. Book IV, Ch. III
22. Piepenbrock M-OM, Lloyd GO, Clarke N, Steed JW (2010) Chem Rev 110:1960
23. (a) Marsella MJ, Reid RJ, Estassi S, Wang L-S (2002) J Am Chem Soc 124:12507; (b) Lee Y-A, Eisenberg R (2003) J Am Chem Soc 125:7778; (c) Beyer MK, Clausen-Schaumann H (2005) Chem Rev 105:2921; (d) Ahir SV, Terentjev EM (2005) Nat Mater 4:491; (e) Zanuy D, Aleman C (2007) Chem Eur J 13:2695; (f) Kobatake S, Takami S, Muto H, Ishikawa T, Irie M (2007) Nature 446:778
24. (a) Wiedemann G, Schmidt F (1895) Ann Phys (Leipzig) 54:604; (b) Walton AJ (1977) Adv Phys 26:887; (c) Zink JI (1978) Acc Chem Res 11:289
25. (a) Verezub NV, Krauya UÉ, Kalnin PP, Lavrinenko SN (1991) Mech Compos Mater 27:207; (b) Sage I, Badcock R, Humberstone L, Geddes N, Kemp M, Bourhill G (1999) Smart Mater Struct 8:504; (c) Sage I, Bourhill G (2001) J Mater Chem 11:231; (d) Bourhill G, Palsson LO, Samuel IDW, Sage IC, Oswald IDH, Duignan JP (2001) Chem Phys Lett 336:234–241
26. (a) Hardy GE, Kaska WC, Chandra BP, Zink JI (1981) J Am Chem Soc 103:1074; (b) Sweeting LM, Rheingold AL (1987) J Am Chem Soc 109:2652; (c) Rheingold AL, King W (1989) Inorg Chem 28:1715; (d) Antipin VA, Voloshin AI, Ostakhov SS, Kazakov VP (1996) Russ Chem Bull 45:1099; (e) Reynolds GT (1997) J Lumin 75:295; (f) Takada N, Sugiyama J, Minami N, Hieda S (1997) Mol Cryst Liq Cryst 295:71; (g) Akiyama M, Xu C-N, Nonaka K, Watanabe T (1998) Appl Phys Lett 73:3046; (h) Xu C-N, Watanabe T, Akiyama M, Zheng XG (1999) Appl Phys Lett 74:2414; (i) Chen X-F, Zhu X-H, Xu Y-H, Shanmuga Sundara Raj S, Öztürk S, Fun H-K, Ma J, You X-Z (1999) J Mater Chem 9:2919; (j) Liu Y, Xu C-N, Matsui H, Imamura T, Watanabe T (2000) J Lumin 87–89:1297; (k) Zeng X-R, Xiong R-G, You X-Z, Cheung K-K (2000) Inorg Commun 3:341; (l) Chen X-F, Duan C-Y, Zhu X-H, You X-Z (2001) Mater Chem Phys 72:11; (m) Zarkhin LS (2002) Polymer Sci Sri A 44:992; (n) Soares-Santos PCR, Nogueira HIS, Almeida Paz FA, Sá Ferreira RA, Carlos LD, Klinowski J, Trindade T (2003) Eur J Inorg Chem 3609; (o) Ronfard-Haret JC (2003) J Lumin 104:103; (p) Bulgakov RG, Kuleshov SP, Zuzlov AN, Vafin RR (2004) Russ Chem Bull Int Ed53:2712; (q) Jia Y, Yei M, Jia W (2006) Opt Mater 28:974; (r) Bukvetskii BV, Mirochnik AG, Zhikhareva PA, Karasev VE (2006) J Struct Chem 47:575; (s) Li X-L, Zheng Y, Zuo J-L, Song Y, You X-Z (2007) Polyhedron 26:5257; (t) Chandra BP (2008) J Lumin 128:1217; (u) Bergeron NP, Hollerman WA, Goedeke SM, Moore RJ (2008) Int J Impact Eng 35:1587
27. Chen X-F, Zhu X-H, Xu Y-H, Shanmuga Sundararaj S, Öztürk S, Fun H-K, Ma J, You X-Z (1999) J Mater Chem 9:2919
28. Feffrey GA (1973) Carbohyfrate Res 28:233
29. Armstrong HE, Lowry M (1903) Proc R Soc Lond 72:258
30. Andrews TWS (1910) J Ind Eng Chem 478.
31. Egerton ACG, Woolwich RMA (1911) Nature 85:308

32. (a) Hasegawa M, Ishii A, Kishi S (2006) J Photochem Photobiol 178:220;(b) Hasegawa M, Ohmagari H (2020) Chem Lett 49:845; (c) Hasegawa M (2022) Lanthanide luminescence enhancement in nanostructures by coordination chemistry. In: Ntwaeaborwa OM (ed) Luminescent nanomaterials. E-book, Jenny Stanford Publishing Pte. Ltd. ISBN: 9789814968119
33. (a) Bünzli J-C (2006) Acc Chem Res 39:51; (b) Binnemans K (2015) Coord Chem Rev 295:1; (c) Hasegawa Y, Wada Y, Yanagida S (2004) J Photochem Photobiol C 5:183
34. Dexter DL (1953) J Chem Phys 21:836
35. Förster T (1948) Ann Phys 437:55
36. Chow CY, Eliseeva SV, Trivedi ER, Nguyen TN, Kampf JW, Petoud S, Pecoraro VL (2016) J Am Chem Soc 138:5100
37. (a) Terasaki N, Xu C-N, Imai Y, Yamada H (2007) Jpn J Appl Phys 46:2385; (b) Li C, Xu CN, Zhang L, Yamada H, Imai Y (2008) J Visualization 11:329
38. (a) Xu CN, Zheng XG, Watanabe T, Akiyama M, Usui I (1999) Thin Solid Films 352:273; (b) Palumbo DT, Brown JJ, Jr (1970) J Electrochem Soc 117:1184; (c) Zhang Y, Ma L, Wang K, Xu X, Gao Y, Wen S, Luo J (2017) J Lumin 182:22
39. (a) Tsuboi Y, Seto T, Kitamura N (2008) J Phys Chem 112:6517; (b) Eddingsaas NC, Suslick KS (2006) Nature 444:163; (c) Ilatovskii DA, Tyutkov NA, Vinogradov VV, Vinogradov AV (2018) ACS Omega 3:18803
40. Fontenot ES, Hollerman WA, Aggarwal MD, Bhat KN, Goedeke SM (2012) Measurement 45:431
41. (a) Sage I, Badcock R, Humberstone L, Geddes N, Kemp M, Bourhill G (1999) Smart Mater Struct 8:504; (b) Sage I, Badcock R, Humberstone L, Geddes N, Kemp M, Bishop S, Bourhill G (1999) Proc SPIE-Int Soc Opt Eng 3675:169; (c) İncel A, Emirdag-Eanes M, McMillen CD, Demir MM (2017) ACS Appl Mater Interfaces 9:6488
42. (a) Hasegawa M, Ohmagari H (2020) J Imaging Soc Jpn 59:325; (b) Hasegawa M, Saso A, Yamamoto Y, Ohmagari H, Saito D, Hattori S, Karasawa M, Ito S, Kato M,. Ishii K (2022) (in preparation)
43. Sage I, Bourhill G (2001) J Mater Chem 11:231–245
44. (a) Longchambon H (1925) Bull Soc Fr Miner 48:130; (b) Sodomka L (1971) Phys Status Solidi A 7:K65
45. (a) Meyer K, Polly F (1965) Phys Status Solidi 8:441; (b) Meyer K, Obrikat D, Rossberg M (1970) Krist Tech 5:181
46. (a) Nowak R, Krajewska A, SamocÂ M (1983) Chem Phys Lett 94:270; (b) Tokhmetov AT, Vettegren VI (1989) Sov Phys Sol State 31:2125
47. Chandra BP, Zink JI (1980) Phys Rev B: Solid State 21:816
48. Reynolds GT (1997) J Lumin 75:295
49. Shikha ST, Tiwari S, Sahu BK, Chandra BP (1995) Bull Mater Sci 18:503
50. Hirai Y, Nakanishi T, Kitagawa Y, Fushimi K, Seki T, Ito H, Hasegawa Y (2017) Angew Chem Int Ed 56:7171
51. Hasegawa Y, Tateno S, Yamamoto M, Nakanishi T, Kitagawa Y, Seki T, Ito H, Fushimi K (2017) Chem Eur J 23:2666
52. Hirai Y, Kotani A, Sakaue H, Kitagawa Y, Hasegawa Y (2019) J Phys Chem C 123:27251
53. (a) Chandra BP, Deshmukh NG, Jaiswal AK (1987) Mol Cryst Liq Cryst 142:157; (b) Wolff G, Gross G, Stranski IN (1952) Z Electrochem 56:420.
54. Cotton FA, Daniels LM (2001) Inorg Chem Commun 4:319
55. Chandra BP, Zink JI (1981) J Phys Chem Solids 42:529–532
56. Wong H-Y, Lo W-S, Chan WTK, Law G-L (2017) Inorg Chem 56:5153–5140
57. Li D-P, Li C-H, Wang J, Kang L-C, Wu T, Li Y-Z, You X-Z (2009) Eur. J. Inorg. Chem 4844
58. Bukvetskii BV, Mirochnik AG, Shishov AS (2018) J Lumines 195:44
59. Bukvetskii BV, Mirochnik AG, Zhikhareva PA (2018) Inorg Chim Acta 483:565
60. Xiong R-G, You X-Z (2002) Inorg Chem Commun 5:677–681
61. Mirochnik AG, Shishov AS, Bukvetskii BV (2016) Lumines 31:1329
62. Eliseeva SV, Pleshkov DN, Lyssenko KA, Lepnev LS, Bünzli J-CG, Kuzmina NP (2010) Inorg Chem 49:9300–9311

63. Bukvetskii BV, Kalinovskaya IV (2017) J Fluorec 27:773
64. (a) Sweeting LM (1990) Chem Matt 10–11; (b) Gao G-L, Jia Y-R, Jiang H, Xia M (2021) Dye Pigment 186:109030
65. Kubota K, Pang Y, Miura A, Ito H (2019) Science 366:1500–1504
66. Hasegawa M, Iwasawa D, Kawaguchi T, Koike H, Saso A, Ogata S, Ishii A, Ohmagari H, Iwamura M, Nozaki K (2020) ChemPlusChem 85:294–300
67. Yuan L, Yin M, Yuan E, Sun J, Zhang K (2004) Inorg Chim Acta 357:89
68. Hasegawa Y, Hieda R, Miyata K, Nakagawa T, Kawai T (2011) Eur J Inorg Chem 4978–4984
69. Hirai Y, Paulo Ferreira da Rosa P, Nakanishi T, Kitagawa Y, Fushimi K, Seki T, Ito H, Hasegawa Y (2018) Inorg Chem 57:14653–14659
70. Wu M-Y, Xu J-X, Chen Y-H, Lu I-C, Han J-L, Lin P-H (2022) Dalton Trans 51:69–73
71. Kitagawa Y, Naito A, Fushimi K, Hasegawa Y (2021) Chem Eur J 27:2279–2283
72. Artem'ev AV, Davydova MP, Berezin AS, Sukhikh TS, Samsonenko DG (2021) Inorg Chem Front 8:2261–2270
73. Goodgame DML, Cotton FA, 726 (1961). Phosphine oxide complexes Part V. Tetrahedral complexes of manganese (II) containing triphenylphosphine oxide, and triphenylarsine oxide as ligands. J Chem Soc 3735–3741
74. (a) Matsuzawa T, Aoki Y, Takeuchi N, Murayama Y (1996) J Electrochemical Soc 143:2670–2673; (b) Akiyama M, Xu C-N, Nonaka K, Watanabe T (1998) Appl Phys Lett 73:3046–3048
75. Zhang J-C, Wang X, Marriott G, Xu C-N (2019) Prog Mater Sci 103:678–742
76. Yang F, Yuan Y, Sijbesma RP, Chen Y (2020) Macromoleclues 53:905–912